37th Cement and Concrete Science Conference
11-12 September 2017
University College London
Paper Number 112

Autogenous Shrinkage of Alkali-activated Fly Ash/Slag Paste

Guohao Fang, Mingzhong Zhang
Advanced and Innovative Materials (AIM) Group, Department of Civil, Environmental and Geomatic Engineering, University College London, UK

ABSTRACT

The autogenous shrinkage of alkali-activated fly ash/slag (AAFS) pastes during first 24 h after casting is an important engineering property, as it significantly contributes to ultimate shrinkage and cracking risk. However, the studies on this property are still limited. The objective of this work is to provide a better understanding of autogenous shrinkage of AAFS pastes at very early age (<24 h). The autogenous shrinkage of AAFS pastes with 10%, 20% and 30% slag replacement ratios of fly ash are estimated. A series of tests including workability, setting time and chemical reaction tests are conducted to investigate shrinkage mechanism of AAFS pastes. The results show that the ultimate autogenous shrinkage and the highest shrinkage rate of AAFS pastes increases significantly from 1271 to 1740 με and from 201 to 943 με/h respectively as slag replacement ratio increases from 10% to 30%. This is likely because the additional slag contents accelerate the formation of aluminosilicate gels and result in reorganization and rearrangement of microstructures. Additionally, AAFS paste with a larger autogenous shrinkage exhibits a worse workability and shorter setting time. The different reaction processes lead to the different early-age autogenous shrinkage of these AAFS mixtures.

1. INTRODUCTION

Alkali-activated fly ash/slag (AAFS) is a new blended alkali-activated materials (AAM) that has been increasingly studied over the past decades owing to its environmental benefits and superior engineering properties, e.g., mechanical properties and chemical durability. Despite its superior mechanical and eco-friendly performance, the practical applications of AAFS remain low mainly due to the uncertain long-term durability and insufficient ability against shrinkage and micro-cracking [1].

Shrinkage is an important engineering property of AAM that can affect the cracking probability and thus durability of AAM by providing easy access to water and aggressive species into the interior of concrete [2]. Many studies to date report that AAM have significantly higher autogenous and drying shrinkage than ordinary Portland cement (OPC) [3]. It is also found that the shrinkage of AAM is influenced by different factors, such as chemical and physical properties of binder, activator species and dosage, and curing conditions [4]. However, the investigations on shrinkage, particularly autogenous shrinkage of AAFS are still limited. Autogenous shrinkage is a volume change resulting when there is no moisture transfer to the surrounding environment. It is attributed to chemical reactions and internal structural changes. Although the autogenous shrinkage of AAFS at older ages has been documented and explained by self-desiccation, the presence of autogenous shrinkage during the first day after casting still lack of theoretical explanation [4].

During first 24 h, the AAFS pastes will transform from liquid stage to hardened stage. This transition is very important concerning the initiation of autogenous shrinkage strain and induced stress, which significantly contribute to ultimate shrinkage and cracking risk. Therefore, it is of importance to measure the autogenous shrinkage immediately after casting in order to fully understand the mechanism causing autogenous shrinkage of AAFS pastes.

The objective of this study is to provide a better understanding of the early-age autogenous shrinkage of AAFS pastes. The autogenous shrinkage of AAFS pastes with slag content as 10%, 20% and 30% of total binder at early 24 h after casting is studied. A series of tests such as workability, setting time and chemical reaction tests are conducted to investigate the shrinkage mechanism of AAFS pastes.

2. EXPERIMENTAL PROGRAM

2.1. MATERIALS

In this study, class F fly ash (FA) and ground granulated blast-furnace slag (GGBS) were used as binder materials. The chemical compositions of FA and GGBS are listed in Table 1. The mean particle size of FA and GGBS is 26.81 and 14.77 μm, respectively. The alkaline activator was prepared by mixing sodium hydroxide (>98% purity) with distilled water and sodium silicate solution. The concentration of sodium hydroxide (SH) was 10 M for all mixtures. The mass ratio of SiO_2 to Na_2O of sodium silicate (SS) was 2.0 with chemical composition of 30.71 wt.% SiO_2, 15.36 wt.% Na_2O and 53.93 wt.% H_2O. The modified polycarboxylate based superplasticizers (SPs) were used to improve the workability of AAFS pastes.

Table 1. Chemical compositions (wt.%) of FA and GGBS

Oxide	SiO_2	Al_2O_3	CaO	Fe_2O_3	MgO
FA	53.24	26.42	3.65	9.55	1.65
GGBS	36.7	13.56	37.6	0.41	7.45

2.2. MIXTURE PROPORTIONS OF PASTE

The AAFS pastes with three different GGBS replacement ratios for FA were designed and tested in this work. The mixture proportions of AAFS paste are given in Table 2 and denoted with specific codes. The label 'FS' represents AAFS paste, while the number, '10', '20', or '30', stands for the percentage of GGBS replacement for FA by weight. The ratio of alkaline activator to binder by weight (AL/B) was 0.4. The mass ratio of sodium silicate to sodium hydroxide (SS/SH) was 2.0. In addition, the mass ratio of SPs to binder (B) was 0.01.

Table 2. Mixture proportions of the AAFS paste

Mixtures	AL/B	FA/GGBS	SS/SH	SPs/B
FS10	0.4	90/10	2.0	0.01
FS20	0.4	80/20	2.0	0.01
FS30	0.4	70/30	2.0	0.01

2.3. TESTING METHODS

The early-age autogenous shrinkage was measured with the help of a non-contact method with laser displacement sensors. As shown in Figure 1, the specimen setup for autogenous shrinkage measurement consists of two elements: 1) a PVC mould with a seal cover, whose inner size is 70×70×70 mm; and 2) an envelope formed by two PVC plates (i.e., reflecting plates) and a plastic sheet. Oil was spread between the plastic sheet and the mould to limit friction between paste specimen and mould. The freshly mixed AAFS pastes was cast into the envelope positioned in the mould. The top of mould was then sealed by a plastic sheet and covered by a thick PVC plate to limit the water evaporation of paste. After that, the mould was placed in the shrinkage testing chamber with a constant temperature of 20 ± 3 °C and relative humidity of 40%. When the paste specimen shrinks, the reflecting plates were dragged along by the paste. A laser sensor with measuring accuracy of 0.001 μm was used to detect the reflecting plate's displacement, from which the horizontal deformation of specimen (i.e., autogenous shrinkage) can be calculated (see Figure 2). The trials indicated that the displacement of two plates are almost the same. Thus, only one side's displacement was measured and used to calculate the whole horizontal deformation. The data of shrinkage were logged on a computer at 0.2 s interval for a period of 24 h. To ensure the reproducibility, three duplicate samples were prepared to obtain the mean value of autogenous shrinkage.

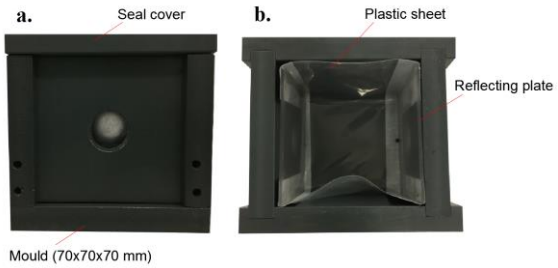

Figure 1. Autogenous shrinkage measurement mould: (a) side view of mould; (b) internal view of mould

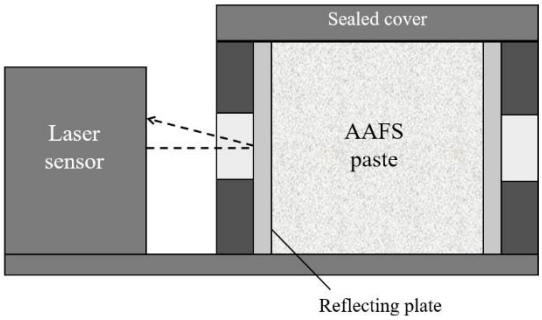

Figure 2. Schematic section view of autogenous shrinkage measurement.

In addition, a series of tests were conducted to study the shrinkage mechanism of AAFS pastes at early age in detail. The flow table spread test according to ASTM C230 was used to investigate the effect of workability on evolution of autogenous shrinkage at liquid stage. The Vicat setting test was applied to explore the relationship between setting time and shrinkage

development in transition stage, which was determined according to ASTM C191. Finally, the chemical reaction of AAFS pastes at early 24 h was studied to explain the evolution process of autogenous shrinkage, which was determined at 20 °C with an isothermal calorimetry (TAM Air model, TA instruments, USA).

3. RESULTS

Figure 3 shows the autogenous shrinkage of three different sealed AAFS pastes at early 24 h after casting. The development of autogenous shrinkage at this period can be divided into three stages, including liquid, transition and rigid stages (see FS20 in Figure 3). The label 'A1', 'B1' and 'C1' represent the critical shrinkage values of FS10, FS20 and FS30 in liquid stage respectively, while 'A2', 'B2' and 'C2' refer to the critical shrinkage values in transition stage. As seen in Figure 3, the autogenous shrinkage increases dramatically in liquid stage but becomes slower in transition stage. After that the shrinkage keeps stable for several hours in early rigid stage but increases again in later rigid stage.

More specifically, it can be found that the increase of autogenous shrinkage of FS30 is faster than that of FS20 and FS10 in liquid stage. The critical shrinkage value of FS30 (C1-942 με) occurs at about 1 h after casting, while those of FS20 (B1-1100 με) and FS10 (A1-900 με) occur at about 1.5 h and 7 h, respectively. Similarly, the shrinkage development of FS30 in transition stage is also faster than FS20 and FS10. For FS30, it takes about 2 h from C1 (942 με) to C2 (1400 με), while FS20 and FS10 take about 3 h and 4 h respectively from B1 (1100 με) to B2 (1300 με) and from A1 (900 με) to A2 (1150 με). In addition, the ultimate autogenous shrinkage of FS30 (1740 με) in rigid stage is higher than those of FS20 (1457 με) and FS10 (1271 με). It indicates that the addition of GGBS would accelerate and increase the autogenous shrinkage of AAFS pastes at early age and the effect of GGBS at 20% replacement level appears to be more pronounced.

The kinetic of autogenous shrinkage for different AAFS paste is shown in Figure 4. It can be found that the highest autogenous shrinkage rates of FS30 (942 με/h) and FS20 (696 με/h) occur at 1 h after casting. However, the appearance of the highest shrinkage rate of FS10 is lower than those of other two samples and tends to be delayed. The highest shrinkage rate of FS10 (201 με/h) occurs after 2 h. It indicates that the kinetic of autogenous shrinkage of AAFS pastes is highly dependent on the content of GGBS.

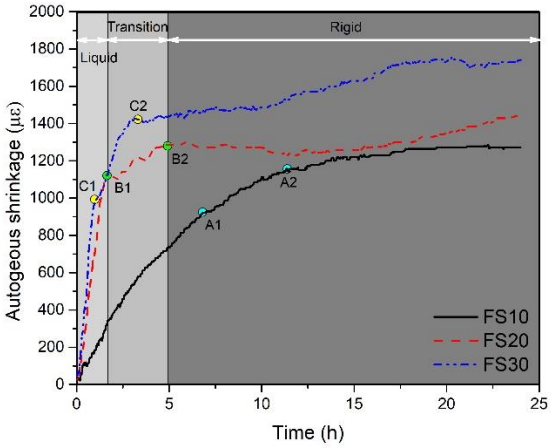

Figure 3. Autogenous shrinkage of different AAFS pastes

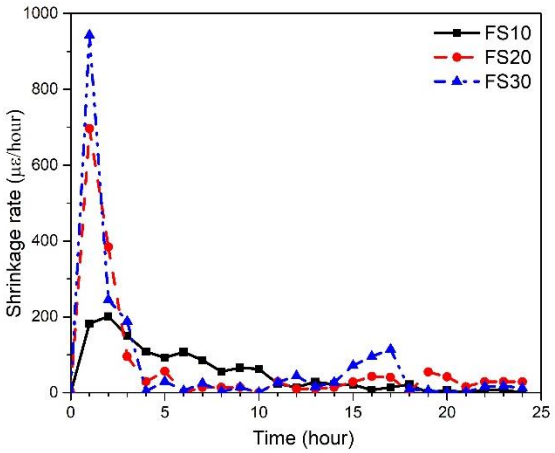

Figure 4. Kinetics of autogenous shrinkage of different AAFS pastes

4. DISCUSSION

In this work, the early-age autogenous shrinkage is defined as the horizontal deformation occurring immediately after paste placing up to the age of 24 h. This period mainly consists of three stages, i.e., the time when the paste is fluid or liquid, the transition period when the skeleton of paste is formed to create early stiffness, and the initial hardening stage when the paste is rigid. Thus, the shrinkage mechanism of AAFS pastes is subsequently discussed according to different stages.

During the very early phase while the paste is still liquid, there is no skeleton formed from reaction to hold the body firmly in place. Any movement of the paste due to the applied stress would be immediately shifted. Thus, the deformation of AAFS paste in this period is mainly affected by its workability. As shown in Figure 5, the flow value of AAFS paste decreases with the increase of GGBS content. Comparing with the results of autogenous shrinkage, the paste with a better workability shows a lower autogenous shrinkage.

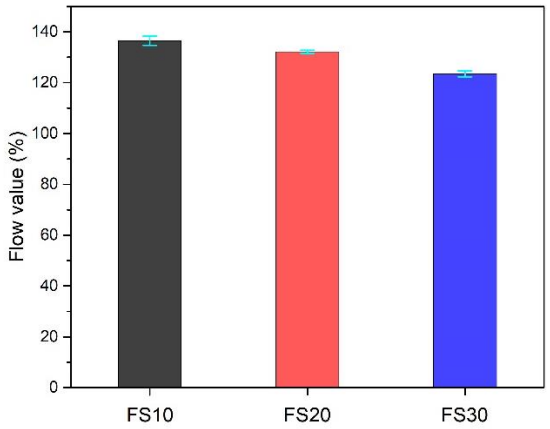

Figure 5. Workability of different AAFS pastes

After the binder and activator have begun to react, a skeleton would form due to the formation of reaction products. During this phase, the capillary pressure would start to develop and cause shrinkage in transition stage. In addition, the setting time would also occur as a result of paste stiffening. As shown in Figure 6, the paste with highest slag content (FS30) has shortest setting time, which means that it is prior to create shrinkage in transition stage. The results suggest that the AAFS paste with shorter setting time would accelerate shrinkage process.

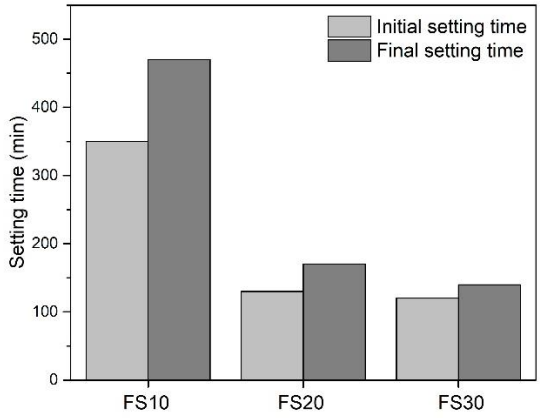

Figure 6. Setting time of different AAFS pastes

Once the skeleton is well established the paste often has sufficient strength to resist additional stresses. The shrinkage rate would be slowed and tends to 0 because the paste can withstand some driving forces (see FS10 in Figure 4). However, it is found that the shrinkage rates of FS20 and FS30 increase again after 14 h (see Figure 4). This is likely because the increase of GGBS content promotes the continuous formation of reaction products, e.g., aluminosilicate gels (see Figure 7). The generation of reaction products would then increase the dissolution of binder and provide the driving force. Thus, the continuous reaction may result in the reorganization and rearrangement of the aluminosilicate gel structure and cause further autogenous shrinkage during the rigid stage.

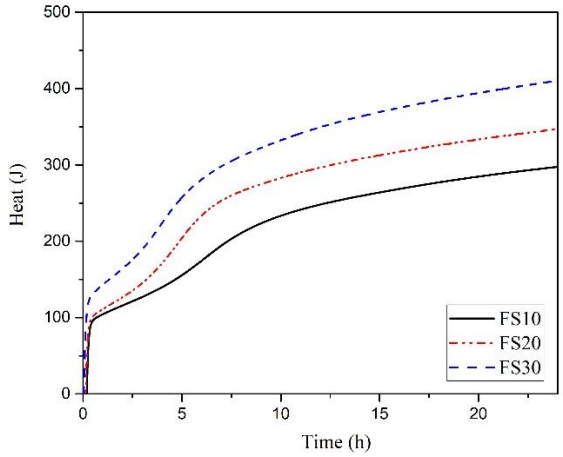

Figure 7. Cumulative heat of different AAFS pastes

5. CONCLUSIONS

In this study, the early-age autogenous shrinkage of AAFS pastes was investigated in a quantitative manner. Based on the experimental results, the main conclusions can be drawn as follows:

- The development of autogenous shrinkage of AAFS paste can be divided into three stages: liquid, transition and rigid stages.
- The addition of GGBS would accelerate and increase the early-age autogenous shrinkage of AAFS pastes. The effect of GGBS at 20% replacement level appears to be more pronounced.
- The larger autogenous shrinkage can be attributed to the reorganization and rearrangement of microstructure due to continuous formation of reaction products.

REFERENCES

[1] I. Ismail, S.A. Bernal, J.L. Provis, R. San Nicolas, S. Hamdan, J.S.J. van Deventer, 2014. Modification of phase evolution in alkali-activated blast furnace slag by the incorporation of fly ash, *Cem. Concr. Comp*, 45 125-135.
[2] H. Ye, A. Radlińska, 2016. Shrinkage mechanisms of alkali-activated slag, *Cem. Concr. Res.*, 88 126-135.
[3] Y. Ma, G. Ye, 2015. The shrinkage of alkali activated fly ash, *Cem. Concr. Res*, 68 75-82.
[4] A.A. Melo Neto, M.A. Cincotto, W. Repette, 2008. Drying and autogenous shrinkage of pastes and mortars with activated slag cement, *Cem. Concr. Res*, 38 (4) 565-574.